Journal of Alloys and Compounds 495 (2010) 82–87

Contents lists available at ScienceDirect

Journal of Alloys and Compounds

journal homepage: www.elsevier.com/locate/jallcom

Preparation of 3D rose-like NiO complex structure and its electrochemical property

Ling Wang, Yan Zhao, Qiongyu Lai*, Yanjing Hao

College of Chemistry, Sichuan University, Chengdu 610064, PR China

ARTICLE INFO

Article history:
Received 30 November 2009
Received in revised form 14 January 2010
Accepted 19 January 2010
Available online 25 January 2010

Keywords:
Electrode material
Oxide material
Chemical synthesis
Crystal growth

ABSTRACT

The reaction of nickel chloride and sodium acetate under solvothermal conditions produced $Ni(OH)_2$ nanoplatelets, which are self-assembled to form a 3D rose-like morphology. After calcination, NiO nanoplatelets were obtained and inherited the rose-like morphology of $Ni(OH)_2$ precursor. The influences of PEG and reaction temperature on the size and morphology of NiO were investigated. The functions of PEG on the formation of the NiO nanoplatelets and the self-assembly process were discussed. Moreover, the possible mechanism for the formation of rose-like morphology was proposed. The cyclic voltammetry (CV) measurement showed that as-prepared NiO with a rose-like morphology exhibited a good pseudo-capacitance behavior.

1. Introduction

NiO nanomaterials have received intensive attention due to their attractive applications in diverse fields, such as electrode materials [1], magnetic materials [2], optical materials [3], catalysts [4] and gas sensors [5]. Of fundamental importance is the preparation of NiO nanomaterials with novel morphologies because the size and shape are intimately related to their properties and applications. It has been established that size and morphology of NiO products can be controlled by using the different preparation methods. For examples, NiO nanoparticles were prepared by anodic arc plasma method [6]. NiO nanowires were successfully prepared via a wet chemical method [7]; NiO nanorolls could be selectively synthesized through a facile hydrothermal synthetic method [8]; NiO nanowalls were obtained by using a plasma assisted oxidation method [9]; NiO nanotubes had been produced for the first time via an anodic aluminium oxide (AAO) template processing method [10].

In nanomaterials science, 3D complex structure self-assembled by single nanoparticles has become an attention focus because of its unique properties and potential applications. Wang et al. reported that $Ni(OH)_2$ hollow microspheres with $Ni(OH)_2$ nanosheets as the in situ formed building units were prepared via a novel template-free approach [11]. Coudun and Hochepied obtained $Ni(OH)_2$ with a "stack of pancakes" morphology by the dual function of ammonia and template [12]. Kuang et al. demonstrated that hierarchical β-$Ni(OH)_2$ microspheres self-assembled from nanosheets building blocks were successfully fabricated via a hydrothermal process [13]. Cao et al. indicated that self-assembled 3D nanostructures α- and β-$Ni(OH)_2$ were prepared in a water-in-oil reverse microemulsion system [14]. However, to the best of our knowledge, few reports have concerned the synthesis of 3D rose-like NiO via chemical regulation under solvothermal conditions.

Herein, we report the preparation of the self-assembled 3D rose-like microstructures of NiO by chemical regulation under solvothermal conditions, involving complexation–dissociation equilibrium, hydrolysis equilibrium and precipitation–dissolution equilibrium. The effects of PEG and reaction temperature on the size and morphology of samples were also investigated. Moreover, the possible growth mechanism of the rose-like NiO was proposed and discussed. As an example of applications, the obtained 3D rose-like NiO as electrode material showed a good pseudo-capacitance behavior.

2. Experimental

2.1. Preparation

All the chemicals were purchased and used as received without further purification. In a typical synthesis, 0.5348 g of $NiCl_2 \cdot 6H_2O$ was dissolved in 17 mL of ethylene glycol (EG) to form a clear light green solution, then 1.62 g of sodium acetate (NaAc), 0.45 g of PEG4000 and 1 mL of deionized water were sequentially added into the above solution under vigorous stirring and heated to get a clear light green solution. The resulting solution was transferred to a 25 mL Teflon-lined stainless-steel autoclave and heated at 190 °C for 8 h, and then cooled naturally to room temperature. The green product was collected by filtration, washed by ethanol and dried at 60 °C for 3 h. The green product was then immersed in a 6 mol/L KOH solution for 10 h,

* Corresponding author. Tel.: +86 28 85416969; fax: +86 28 85416969.
E-mail address: laiqy5@hotmail.com (Q.Y. Lai).

0925-8388/$ – see front matter © 2010 Elsevier B.V. All rights reserved.
doi:10.1016/j.jallcom.2010.01.091

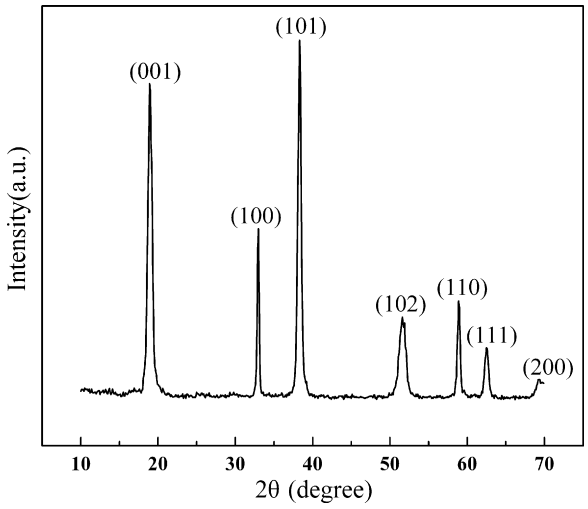

Fig. 1. XRD pattern of $Ni(OH)_2$ precursor sample.

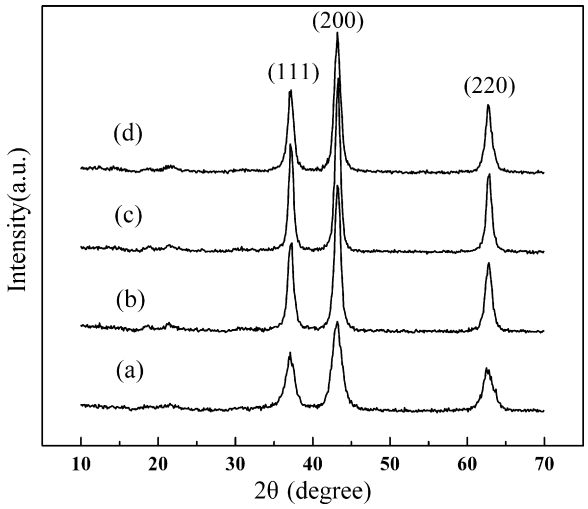

Fig. 2. XRD patterns of NiO samples obtained at 190 °C: (a) without adding PEG; (b) adding PEG400; (c) adding PEG4000; (d) adding PEG10000.

and washed till to be neutral. After the green product was dried at 60 °C for 6 h, rose-like $Ni(OH)_2$ was obtained. The rose-like NiO could be acquired by calcining the obtained $Ni(OH)_2$ powder at 400 °C for 2 h.

2.2. Characterization

Powder XRD data were collected on a Rigaku D/MAX-rA diffractometer with Cu Kα radiation (λ = 0.15418 nm) being operated at 40 kV and 100 mA. The SEM images were taken on a Hitachi S-450 electron microscope.

2.3. Cyclic voltammetry (CV) measurements

Nickel oxide electrodes were prepared by pressing an active paste into a nickel foam substrate. The paste contained 70 wt% rose-like nickel oxide, 25 wt% acetylene black and 5 wt% polyvinylidene fluoride (PVDF), which were dissolved by N-methyl-2-pyrrolidine (NMP). First, the paste was dried in vacuum at 60 °C for 12 h. Second, the active paste was pressed into a nickel foam substrate that served as a current collector (surface was 1 cm^2) under a pressure of 20 Mpa. Then the nickel oxide electrodes were dried in a vacuum at 60 °C for 3 h. The CV tests were performed with a three-electrode cell equipped with a working electrode, a platinum foil counter electrode and a saturated calomel reference electrode (SCE), and carried out with LK2005 electrochemical workstation system. The CV measurements were carried out in 6 mol/L KOH solution at room temperature.

3. Results and discussion

3.1. XRD of $Ni(OH)_2$ precursor

Fig. 1 shows the XRD pattern of $Ni(OH)_2$ precursor which was synthesized in the presence of PEG4000 at 190 °C for 8 h and has a hexagonal structure. The peaks at 19.3°, 33.1°, 38.5°, 52.1°, 59.1°, 62.7° and 69.3° could be attributed to the (0 0 1), (1 0 0), (1 0 1), (1 0 2), (1 1 0), (1 1 1) and (2 0 0) planes, respectively [JCPDS Card No. 14-0117]. No diffraction peaks of any impurity phase are detected in the XRD pattern.

3.2. Influences of PEG

All the NiO samples were obtained by calcining the $Ni(OH)_2$ precursor at 400 °C for 2 h. Fig. 2 shows the XRD patterns of different NiO samples prepared without adding PEG (Fig. 2a), with PEG400 (Fig. 2b), PEG4000 (Fig. 2c) and PEG10000 (Fig. 2d). The diffraction peaks at the positions of 37.2°, 43.3° and 62.9° are corresponding to the (1 1 1), (2 0 0) and (2 2 0) planes, respectively. These peaks can be indexed perfectly to cubic NiO phase and are in good agreement with the data of JCPDS file No. 47-1049. Among the four NiO samples, the diffraction peaks in Fig. 2c have the strongest intensity and the sharpest shape, indicating that the sample prepared in the presence of PEG4000 has the best crystallization.

SEM was used to observe the grain morphology and particle size of prepared NiO samples. From Fig. 3a and b, we can see that NiO samples without PEG exhibit lamellar morphology and each slice has small surface area. The prepared NiO nanoplatelets are so thick that they cannot curve and aggregate into flower-like structure. Fig. 3c and d shows that NiO nanoplatelets become large and thin in the presence of PEG400, which tend to incurvate and form flower-like complex structure. Fig. 3e and g shows the overall morphologies of the as-obtained rose-like NiO samples by the addition of PEG4000 and PEG10000, respectively, indicating that the individual flakes are curved and connect to each other through the center to form rose-like architectures with the size of about 2.5 μm in diameter. From the magnification images of the rose-like NiO in Fig. 3f and h, it is revealed that the entire architecture is built from nanoplatelets with smooth surfaces. The thickness of these nanoplatelets is about 70 nm and they connect to each other to form 3D rose-like structures. Based on these results, it is clear that PEG has a significant influence on the morphologies of the products. Without PEG only patch product of NiO was produced. However, when PEG with the appropriate molecular weight was chosen as the surfactant, the rose-like morphology could be obtained.

3.3. Influences of reaction temperature

The samples prepared under the solvothermal condition of 100 °C, 140 °C and 190 °C were respectively calcined at 400 °C for 2 h. Fig. 4 shows the XRD patterns of NiO samples treated at different reaction temperatures. All the NiO samples were synthesized in the presence of PEG4000. The diffraction peaks at 37.2°, 43.3° and 62.9° could be assigned to the (1 1 1), (2 0 0) and (2 2 0) planes of cubic-phased NiO [JCPDS Card No. 47-1049], respectively. No other phase has been observed in the diffraction patterns, indicating that $Ni(OH)_2$ precursor has completely transformed into cubic-phased NiO after calcination at 400 °C for 2 h. It should be noted that among the three NiO samples, the diffraction intensity of the sample synthesized at 190 °C is the strongest and the half-peak width is the narrowest, indicating the product synthesized at this temperature has the highest degree of crystalline character.

Reaction temperature can also affect the morphology of NiO particles. Fig. 5 shows the SEM images of NiO samples synthesized with PEG4000 as the surfactant at different reaction temperatures. Fig. 5b, d and f is the magnification images of Fig. 5a, c and e, respectively. We can see that the rod-like NiO sample can be obtained at the reaction temperature of 100 °C. When the

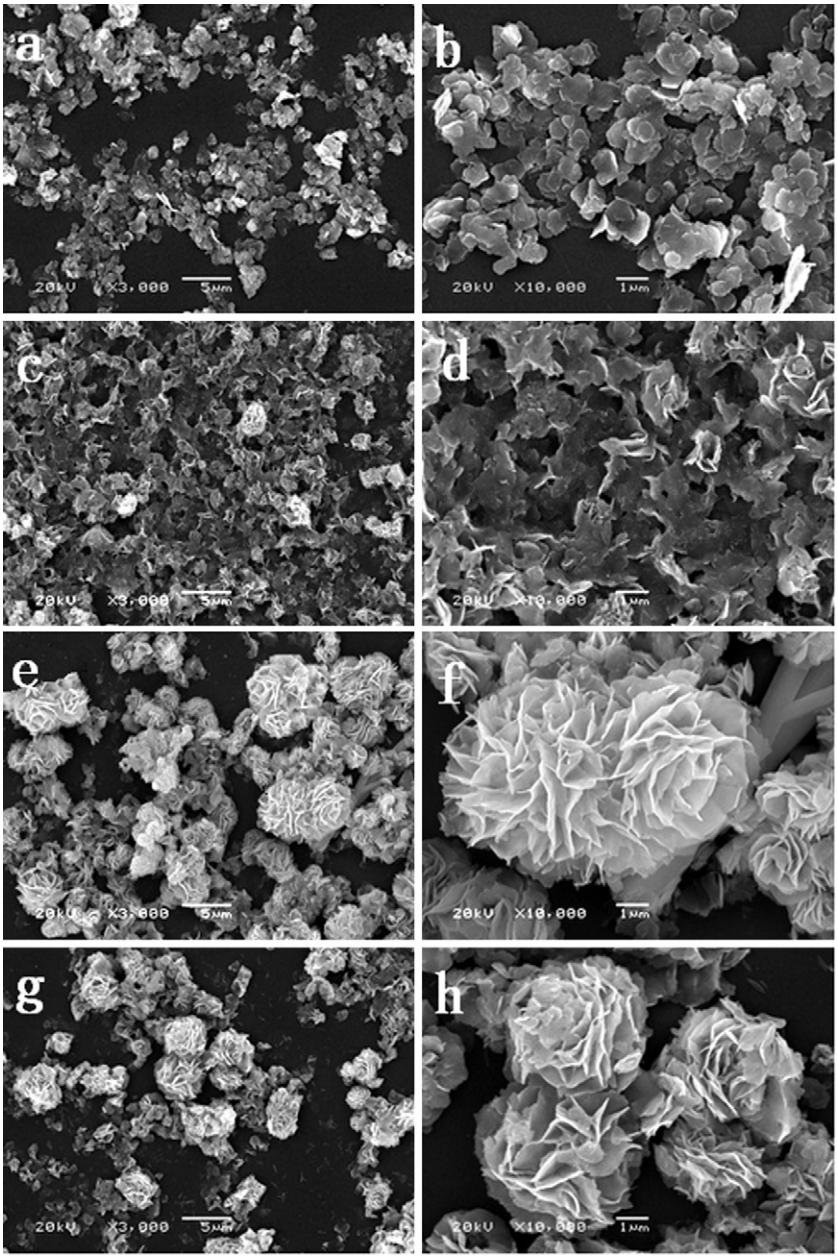

Fig. 3. SEM images of NiO samples obtained at 190 °C (a, b) without adding PEG; (c, d) adding PEG400; (e, f) adding PEG4000; (g, h) adding PEG10000.

solvothermal reaction temperature was up to 140 °C, the morphology of sample changed, and the rod-like and rose-like NiO products were obtained simultaneously. When the reaction temperature further increased to 190 °C, rose-like NiO sample composed of nanoplatelets appeared as the main product. It seems that lower synthetic temperature favors the formation of rod-like NiO product and the higher synthetic temperature favors the formation of well-crystallized NiO phase with rose-like morphology.

3.4. Growth mechanism of the rose-like NiO

In general, the crystal formation process in a solution is mainly divided into two stages: nucleation and crystal growth. In the nucleation process, the special crystal structure and symmetry determine its inherent morphology, which is a key factor to control the crystal morphology [15]. In contrast, crystal growth is a thermodynamically and dynamically controlled process. Crystal seeds, which maintain their inherent shape in some extent, can grow into 1D or other complex structures by controlling reaction conditions such as temperature, reaction time, concentration, etc. [16–19]. As shown in Fig. 6, the morphology of NiO product is almost the same as that of $Ni(OH)_2$ precursor, indicating that the rose-like morphology can remain well during the calcination process.

It is well known that $Ni(OH)_2$ has a hexagonal layer structure with each Ni atom coordinates with six oxygen atoms. In such layered structure, three oxygen atoms are above the crystal plane, and the other three oxygen atoms are below the crystal plane. Hydrogen atoms solely form “hydrogen layer” and the distance of the adjacent hydrogen atoms is about 1.1 nm. In a certain hydrothermal condition, $Ni(OH)_2$ nanoplatelets are easily formed because of their intrinsic lamellar structure [20]. The nanoplatelets can aggregate into the flower-like morphology through self-assembly process by the driving forces, such as electrostatic and dipolar fields associated with the aggregate, hydrophobic interactions, hydrogen bonds, crystal-face attraction, and van der Waals forces [21]. Based on the experimental results and above discussion, the pos-

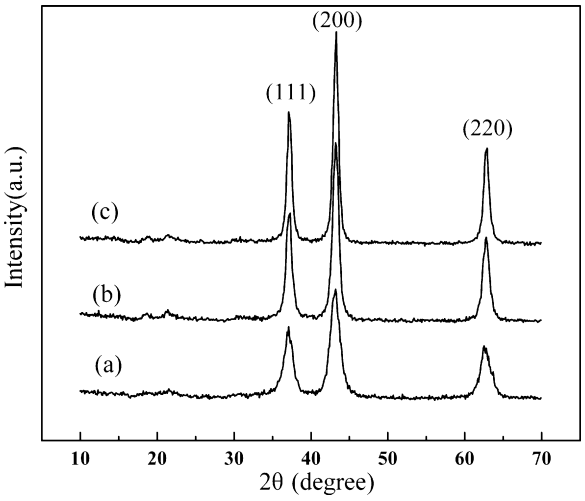

Fig. 4. XRD patterns of NiO samples obtained in the presence of PEG4000 at various reaction temperatures: (a) 100 °C; (b) 140 °C; (c) 190 °C.

sible growth mechanism of the rose-like $Ni(OH)_2$ microstructures has been proposed.

During the formation of $Ni(OH)_2$ nanoplatelets, the related reaction equations can be described as follows, which involve the complexation–dissolution equilibrium, hydrolytsis equilibrium and precipitation–dissolution equilibrium.

$$EG + Ni^{2+} \rightleftharpoons EG - Ni^{2+}\,(\text{complex}) \quad (1)$$

$$CH_3COO^- + H_2O \overset{\text{heating}}{\rightleftharpoons} CH_3COOH + OH^- \quad (2)$$

$$Ni^{2+} + OH^- \rightleftharpoons EG - Ni^{2+}\,(\text{complex}) \quad (3)$$

In the primary stage of the reaction, EG molecules react with Ni^{2+} ions to form coordinated complexes ($EG - Ni^{2+}$) (Eq. (1)) and the hydrolysis of the acetate group provides OH^- ions (Eq. (2)). $Ni(OH)_2$ nuclei are formed instantaneously in solution via the reaction between Ni^{2+} cations and OH^- anions, which are released through complexation–dissociation equilibrium and hydrolysis equilibrium (Eq. (3)). The ions are released slowly through the above-mentioned chemical regulation process, wherefore it is beneficial to form nanoplatelets. From the contrast experiments (Fig. 3), it is found

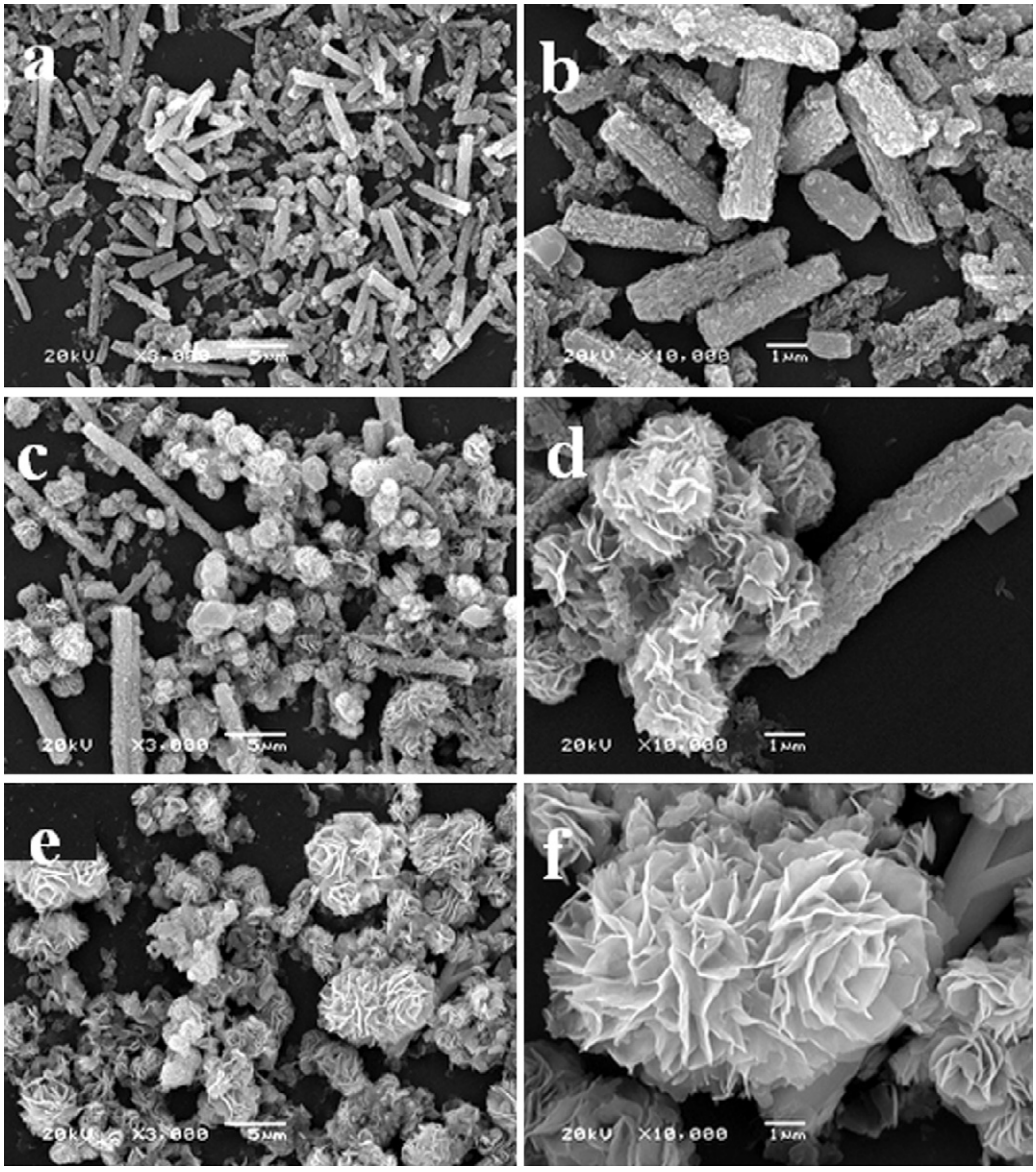

Fig. 5. SEM images of NiO samples obtained in the presence of PEG4000 at various reaction temperatures: (a, b) 100 °C; (c, d) 140 °C; (e, f) 190 °C.

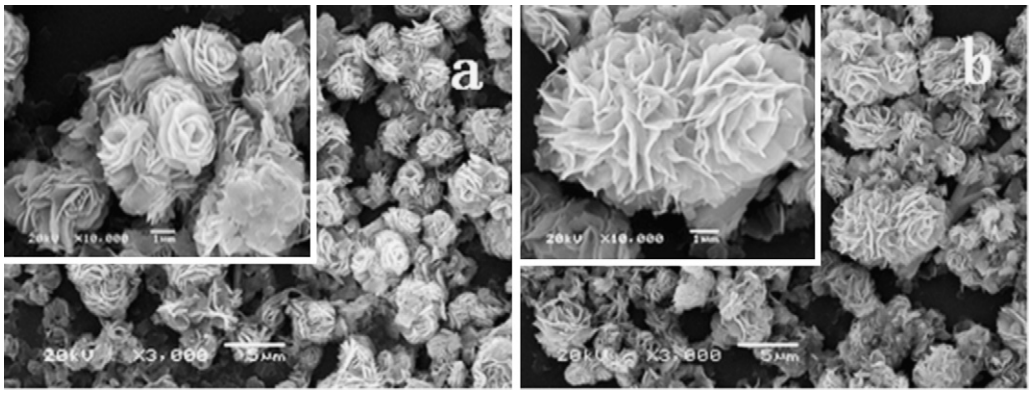

Fig. 6. SEM images of samples prepared in the presence of PEG4000: (a) $Ni(OH)_2$ precursor samples obtained at 190 °C for 8 h; (b) NiO samples obtained from $Ni(OH)_2$ precursor after 400 °C heat treatment. The insets are the magnification images of the corresponding photographs.

that PEG plays a critical role in the formation of the rose-like structure. It is well known that PEG is an excellent surfactant in preparation of shape-controlled nanostructures, since it can selectively adsorb on a certain face of the crystal to minimize the surface energy and accelerate the growth rate of other faces [22]. The molecular weight of PEG has a significant effect on the formation of rose-like structure. The different molecular weight of PEG has different adsorption capacity due to the different chain length and the number of reactive oxygen. Thus, the size and thickness of sheets are not the same, resulting in different degree of curve and aggregation.

Reaction temperature also has a significant influence on the formation of the flower-like structure. When the reaction temperature is low as 100 °C, less Ni^{2+} ions can be released because of the strong coordination between EG and Ni^{2+} ions, leading to the small size nanoplatelets. At the same time, PEG strongly adsorbs on the surface of the nanoplatelets, which prevents the growth of larger sheets. From the viewpoint of crystal growth kinetics, lower temperature is against the nanoplatelets growing into larger sheets. Thus, to decrease their surface energy, the small nanoplatelets spontaneously attached together to generate the rod-like morphology. When the reaction temperature increases up to 190 °C, more Ni^{2+} cations are released due to the weak coordination between EG and Ni^{2+} ions and more OH^- species are generated from the acetate hydrolysis process. As a result, large nanoplatelets are produced. In addition, with the increase of temperature, PEG weakly adsorbs on the crystal surface, making nanoplatelets grow profitably. At the same time, from the viewpoint of crystal growth kinetics, the high temperature is propitious to the growth of large nanoplatelets. These large nanoplatelets are easy to incurvate and aggregate into self-assembled rose-like $Ni(OH)_2$ microstructures.

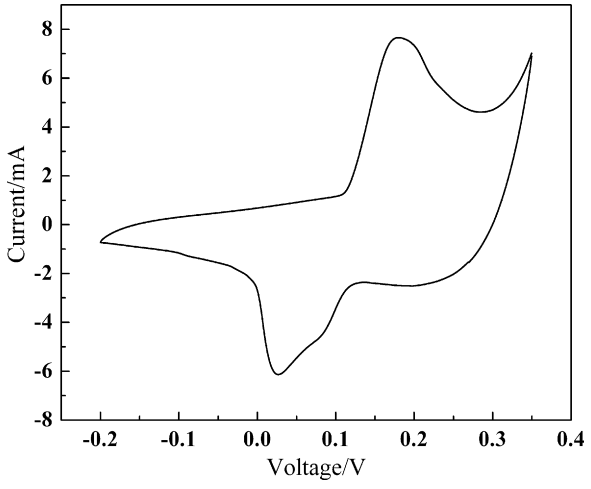

Fig. 7. CV curve of NiO electrode in the potential range of −0.2 to 0.4 V in 6 M KOH solution at a scan rate of 10 mV/s.

3.5. Cyclic voltammetry

The rose-like NiO sample, which was prepared in the presence of PEG4000 at 190 °C, was used as the electrode material for cyclic voltammetry measurement. Fig. 7 shows the CV curve of NiO electrode measured in 6 mol/L KOH electrolyte at a scan rate of 10 mV/s. In the potential range of −0.2 to 0.4 V, two prominent redox peaks appearance and the oxidation and the reduction potential have a shift of around 0.15 V in CV curve, indicating that this process is pseudo-reversible and NiO electrode has good pseudo-capacitance performance. The charge-storage mechanism of NiO for a pseudo-capacitor electrode in alkaline solution has been represented as an invertible oxidation–reduction reaction between Ni^{2+} and Ni^{3+}, which is described by following reaction [23].

$$NiO + zOH^- \underset{\text{discharge}}{\overset{\text{charge}}{\rightleftharpoons}} zNiOOH + (1-z)NiO + ze^- \quad (4)$$

The discharge specific capacitance can be estimated from the voltammetric charge surrounded by the CV curve according to the following formula [24]

$$C = \frac{Q}{\Delta V \times w} = \frac{1}{2\Delta V}\int \frac{I}{vw} dI \quad (5)$$

where C is the specific capacitance of the electrode based on the mass of active materials (F/g), Q is the sum of anodic and cathodic voltammetric charges on positive and negative sweeps (C), I is the current during discharge process (A), ΔV is the potential window of CV (V), v is the scanning rate (V/s) and w is the mass of active electrode materials (g). According to formula (5), the discharge specific capacitance of NiO electrode can be calculated as 87.2 F/g based on the CV curve in Fig. 7. Further investigations of the electrochemical properties are in progress.

4. Conclusions

3D rose-like microstructure of $Ni(OH)_2$ self-assembled from nanoplatelets have been successfully prepared by chemical regulation under solvothermal conditions, involving complexation–dissolution equilibrium, hydrolysis equilibrium and precipitation–dissolution equilibrium. Subsequently, the rose-like NiO nanomaterial was obtained by calcining $Ni(OH)_2$ precursor at 400 °C for 2 h. The results indicated that the molecular

weight of PEG and the reaction temperature would affect the size and morphology of the product. Rose-like NiO is easy to form by using PEG4000 as the surfactant and keeping the reaction temperature at 190 °C under the solvothermal conditions. Cyclic voltammetry measurement shows that the as-prepared rose-like NiO electrode exhibited a good pseudo-capacitance behavior with the discharge specific capacitance of 87.2 F/g.

Acknowledgements

This work is financially supported by the National Natural Science Foundation of China (Grant 20701029). The authors are grateful to X.Y. Ji and X.Y. Zhang at Analytical and Testing Center in Sichuan University for XRD and SEM measurements.

References

[1] X. Wang, L. Li, Y.G. Zhang, S.T. Wang, Z.D. Zhang, L.F. Fei, Y.T. Qian, Cryst. Growth Des. 6 (2006) 2163.
[2] F. Davara, Z. Fereshteha, M. Salavati-Niasari, J. Alloys Compd. 476 (2009) 797.
[3] A.A. Al-Ghamdi, W.E. Mahmoud, S.J. Yaghmour, F.M. Al-Marzouki, J. Alloys Compd. 486 (2009) 9.
[4] Q.L. Zhou, F. Gu, C.Z. Li, J. Alloys Compd. 474 (2009) 358.
[5] G. Mattei, P. Mazzoldi, M.L. Post, D. Buso, M. Guglielmi, A. Martucci, Adv. Mater. 19 (2007) 561.
[6] Z.Q. Wei, H.X. Qiao, H. Yang, C.R. Zhang, X.Y. Yan, J. Alloys Compd. 479 (2009) 855.
[7] C.K. Xu, K.Q. Hong, S. Liu, G.H. Wang, X.N. Zhao, J. Cryst. Growth 255 (2003) 308.
[8] X.H. Liu, G.Z. Qiu, Z. Wang, X.G. Li, Nanotechnology 16 (2005) 1400.
[9] B. Varghese, M.V. Reddy, Y.W. Zhu, C.S. Lit, T.C. Hoong, G.V.S. Rao, B.V.R. Chowdari, A.T.S. Wee, C.T. Lim, C.H. Sow, Chem. Mater. 20 (2008) 3360.
[10] S.A. Needham, G.X. Wang, H.K. Liu, J. Power Sources 159 (2006) 254.
[11] Y. Wang, Q.S. Zhu, H.G. Zhang, Chem. Commun. (2005) 5231.
[12] C. Coudun, J.F. Hochepied, J. Phys. Chem. B 109 (2005) 6069.
[13] D.B. Kuang, B.X. Lei, Y.P. Pan, X.Y. Yu, C.Y. Su, J. Phys. Chem. C 113 (2009) 5508.
[14] M.H. Cao, X.Y. He, J. Chen, C.W. Hu, Cryst. Growth Des. 7 (2007) 170.
[15] Z.A. Peng, X.G. Peng, J. Am. Chem. Soc. 124 (2002) 3343.
[16] Y.W. Jun, S.M. Lee, N.J. Kang, J. Cheon, J. Am. Chem. Soc. 123 (2001) 5150.
[17] Y.H. Kim, Y.W. Jun, B.H. Jun, S.M. Lee, J. Cheon, J. Am. Chem. Soc. 124 (2002) 13656.
[18] V.F. Puntes, D. Zanchet, C.K. Erdonmez, A.P. Alivisatos, J. Am. Chem. Soc. 124 (2002) 12874.
[19] V.F. Puntes, K.M. Krishnan, A.P. Alivisatos, Science 291 (2001) 2115.
[20] J.X. Zhu, Z. Gui, Y.Y. Ding, Z.Z. Wang, Y. Hu, M.Q. Zou, J. Phys. Chem. C 111 (2007) 5622.
[21] L.P. Xu, Y.S. Ding, C.H. Chen, L.L. Zhao, C. Rimkus, R. Joesten, S.L. Suib, Chem. Mater. 20 (2008) 308.
[22] Z.A. Peng, X.G. Peng, J. Am. Chem. Soc. 123 (2001) 1389.
[23] S. Venka, W. John, J. Electrochem Soc. 147 (2000) 880.
[24] C.C. Hu, T.W. Tson, J. Power Sources 115 (2003) 179.